



Crawford, A. O., Cavalli, G., Howlin, B. J., & Hamerton, I. (2016). Improving the hydrolytic stability of aryl cyanate esters by examining the effects of extreme environments on polycyanurate copolymers. *Reactive and Functional Polymers*, 109, 104-111.  
<https://doi.org/10.1016/j.reactfunctpolym.2016.10.007>

Peer reviewed version

License (if available):  
CC BY-NC-ND

Link to published version (if available):  
[10.1016/j.reactfunctpolym.2016.10.007](https://doi.org/10.1016/j.reactfunctpolym.2016.10.007)

[Link to publication record in Explore Bristol Research](#)  
PDF-document

This is the accepted author manuscript (AAM). The final published version (version of record) is available online via Elsevier at <http://dx.doi.org/10.1016/j.reactfunctpolym.2016.10.007>. Please refer to any applicable terms of use of the publisher.

## University of Bristol - Explore Bristol Research

### General rights

This document is made available in accordance with publisher policies. Please cite only the published version using the reference above. Full terms of use are available:  
<http://www.bristol.ac.uk/pure/about/ebr-terms>

# Improving the Hydrolytic Stability of Aryl Cyanate Esters by Examining the Effects of Extreme Environments on Polycyanurate Copolymers

Alasdair O. Crawford<sup>1,†</sup>, Gabriel Cavalli<sup>1</sup>, Brendan J. Howlin<sup>1</sup>, and Ian Hamerton<sup>2,\*</sup>

<sup>1</sup>Department of Chemistry, Faculty of Engineering and Physical Sciences, University of Surrey, Guildford, Surrey, GU2 7XH, U.K.

<sup>2</sup>The Advanced Composites Centre for Innovation and Science, Department of Aerospace Engineering, Queen's Building, University of Bristol, Bristol, BS8 1TR, U.K.

<sup>†</sup> Current address: Henkel Ltd., 957 Buckingham Avenue, Slough, SL1 4NL, U.K.

\* Correspondence to Dr Ian Hamerton, The Advanced Composites Centre for Innovation and Science, Department of Aerospace Engineering, Queen's Building, University of Bristol, Bristol, BS8 1TR, U.K. E-mail: [ian.hamerton@bristol.ac.uk](mailto:ian.hamerton@bristol.ac.uk)

**ABSTRACT:** Three cyanate ester monomer or oligomer species: 2,2-bis(4-cyanatophenyl)propane **1**, 1-1-bis(4-dicyanatophenyl)ethane **2**, and the oligomeric phenolic cyanate **3**, are blended in various ratios to form binary mixtures (18 in total), formulated with copper(II) acetylacetonate (200 ppm) in dodecylphenol (1 % w/v active copper suspension) and cured (3 Kmin<sup>-1</sup> to 150 °C + 1 hour; 3 Kmin<sup>-1</sup> to 200 °C + 3 hours) followed by a post cure (3 Kmin<sup>-1</sup> to 260 °C + 1 hour). Cured copolymers were exposed to environments of elevated relative humidity (75 % RH) and parallel immersion testing in H<sub>2</sub>O, H<sub>2</sub>SO<sub>4</sub> (10 %) and NaOH (10 %) at 25 °C for a period of up to 2 years and accelerated ageing in boiling water (14 days). Periodic measurements are made of moisture gain along with infrared spectra and compared with cured homopolymers. Changes in mass are recorded periodically throughout exposure, prior to destructive thermo-mechanical analyses. Dynamic mechanical thermal analysis data comparing neat and exposed blends demonstrate the detrimental effect of moisture ingress whilst data from thermogravimetric analysis demonstrate no change in degradation onset between neat and exposed materials. An optimised blend of 1:1 of monomer units **1** and **2** was found to absorb less moisture than blends of different stoichiometry or between other respective monomeric units, consequently limiting the deleterious effect of moisture ingress.

**Keywords:** Cyanate Esters, Polymer Blends, Copolymers, Water Absorption, Hydrolysis.

## INTRODUCTION

Thermoset polymers have an established history in civil aviation, in applications involving decorative panels, secondary composite structures and adhesives – around 90 % of the interior furnishings of a typical civil airliner will contain thermoset composites [1]. Cyanate esters (CEs) constitute a family of addition cured high performance, thermosetting polymers, which occupy a niche intermediate between high glass transition temperature ( $T_g$ ), tetrafunctional epoxy resins and bismaleimides (BMIs) [2]. Cured CEs offer a combination of favourable thermal and mechanical performance (*e.g.* dry  $T_g$  values of 270-300 °C are common with a strain at break of over 5-8 %) coupled with low dielectric loss properties (a low dielectric constant of *ca.* 2.7 with a loss tangent of 0.003 (at 25 °C and 1 MHz) is typical) that gives a unique property profile. Although requiring toughening for some engineering applications, CEs can be combined with inherently tough engineering thermoplastics (HexPly 954-2A,  $G_{IC} = 250 \text{ J/m}^2$ ) [3,4] or elastomers (HexPly 953-3,  $G_{IC} = 450 \text{ J/m}^2$ ) [5] to yield impressive enhancements. In this form they typically find application as matrices in advanced composites (either in combination with epoxy resins in aerospace applications [6,7]) or with BMIs as dielectric polymers in the microelectronics industry [8]. Whilst they are not currently widely used in civil aviation, largely due to cost, they are used increasingly in military aerospace applications, *e.g.* the nosecones of aircraft, missile-tracking systems, and weather radar all require resistance to high temperatures, whilst maintaining their electrical properties [9]. Current applications of CEs in radomes and antennae include the Augusta Westland AW101 Merlin helicopter, which uses a Kevlar<sup>TM</sup>/CE sandwich bonded skin [10].

We have previously reported [11] the improvements in physical and mechanical properties that can be achieved by employing binary blends of co-reactive CE monomers. However, little systematic work appears to have been carried out to date with copolymers and we have selected three commonly examined CE monomers based on two bisphenols and a low molecular weight phenolic oligomer. In this study we examine the hydrolytic stability of cured CE copolymers when exposed to water in both mild and increasingly harsh conditions. This has long been a parameter of concern with users of CEs, as the need to achieve high levels of polymer conversion (and thus reduce the presence of cyanate groups that might otherwise yield thermally unstable carbamate groups) is key. We now report success with the potential for CE copolymers, based on commercially available systems, with reduced moisture uptake and superior hydrolytic stability.

## EXPERIMENTAL

**Instrumentation.** Infra-red spectra were obtained (32 scans between 4000-400  $\text{cm}^{-1}$ ) using a Perkin Elmer System 2000 FT-IR spectrometer equipped with diamond ATR.

Differential scanning calorimetry (DSC) was undertaken using a TA Instruments Q1000 running TA Q Series Advantage software on samples ( $5.0 \pm 0.5$  mg) in hermetically sealed aluminium pans. Experiments were conducted at a heating rate of  $10 \text{ Kmin}^{-1}$  from  $-10$  °C to  $400$  °C (heat/cool/heat) under flowing nitrogen ( $50 \text{ cm}^3/\text{min}$ ). In order to gauge the reactivity of the monomer in the bulk, dynamic DSC analysis was performed on all of the systems.

Thermogravimetric analysis (TGA) was performed on a TA Q500 on milled, cured resin samples ( $6.5 \pm 0.5$  mg) in a platinum crucible from  $20$ - $800$  °C at  $10 \text{ Kmin}^{-1}$  in both air and nitrogen ( $40 \text{ cm}^3\text{min}^{-1}$ ).

Dynamic mechanical thermal analysis (DMTA) (in single cantilever mode at a frequency of  $1 \text{ Hz}$ ) was carried out on cured neat resin samples (*ca.*  $3 \times 5 \times 17 \text{ mm}^3$ ) using a TA Q800 in static air from  $20$  °C to  $400$  °C at  $3 \text{ Kmin}^{-1}$  at  $0.1\%$  strain.

**Materials.** The dicyanate ester monomers (Figure 1) were characterised fully using spectroscopic, elemental and thermal analysis and used as received without further purification. The initiator components: copper(II) acetylacetonate ( $\text{Cu}(\text{acac})_2$ ) and dodecylphenol ( $\text{C}_{18}\text{H}_{30}\text{O}$ ) were both obtained from Aldrich and used as received.

Figure 1 Cyanate ester structures studied in this work (*N.B.*, in this instance  $n = 1$  in structure 3)

**Blending and cure of polymer samples for moisture absorption testing.** The  $\text{Cu}(\text{acac})_2 \cdot \text{C}_{18}\text{H}_{30}\text{O}$  initiator suspension ( $1\%$  w/v) was made up by mixing  $\text{Cu}(\text{acac})_2$  with dodecylphenol, heating to  $80$  °C for  $30$  min then ramping to  $120$  °C for a further  $30$  min, stirring throughout. Good homogenisation was achieved.  $\text{Cu}(\text{acac})_2$  ( $200$  ppm) was added to the monomer/s and heated to  $90$  °C whilst stirring to yield a homogenous suspension with uniformly dispersed initiator after *ca.*  $15$  min. The monomer/initiator solution was decanted into aluminium dishes ( $55$  mm diameter, depth  $10$  mm) and cured in a fan-assisted oven heating at  $3 \text{ Kmin}^{-1}$  to  $150$  °C ( $1$  hour isothermal) + heating at  $3 \text{ Kmin}^{-1}$  to  $200$  °C ( $3$  hours isothermal) then post cured - heating at  $3 \text{ Kmin}^{-1}$  to  $260$  °C ( $1$  hour isothermal) followed by a gradual cool ( $3 \text{ K/min}$ ) to room temperature. Cured samples of the different blends (Table 1) were cut to correct size for analysis.

Table 1 Designation of monomers and blends examined in this work

**Conditioning of blends.** An environment of 75 % relative humidity (RH) was created by having NaCl (200 g) in distilled H<sub>2</sub>O (60 ml) held in the base of an air tight, glass container kept at constant temperature for duration of the investigation [12]. Prior to initiation of testing, all blends (17 x 5 x 3 mm<sup>3</sup>) were dried to constant weight in a vacuum oven at 100°C. Blends were then suspended over the NaCl/H<sub>2</sub>O solution on a porous membrane without coming into direct contact with solution. Parallel studies of dried blends of identical size involved directly immersing specimens into either distilled H<sub>2</sub>O, acidic (H<sub>2</sub>SO<sub>4</sub> conc. 10 %) or basic (NaOH conc. 10 %) media in sealed containers to prevent evaporation. These containers were kept at room temperature for the duration of the study. Accelerated testing was performed by immersing similar (dried) samples in distilled water in a round bottom flask with a Leibig condenser and heating at 100 °C for 14 days. Weighing the samples involved removing them from their environment and drying their surfaces. Masses were recorded every 24 hours.

## RESULTS AND DISCUSSION

**Determination of Water Absorption at 75 % RH.** The full series of cured copolymers (in the form of void-free, homogeneous plaques, see Supplementary, Fig. S1) were dried to a constant weight *in vacuo* at 60 °C before being placed in the experimental chamber (75.3 % RH) for 5000 hours with periodic removal for weighing and spectroscopic analysis. The data for each series of blends following exposure to 75.3 % RH are shown in Figure 2(a)-(c); in each case the full data set is presented with the data for the initial period (Figs S2-S4) along with the tabulated changes in sample masses (Table S1) supplied as Supplementary information. None of the samples, which are comparatively thick (3 mm), reach full equilibrium, but the intention was to conduct dynamic mechanical thermal analysis (DMTA) measurements on the conditioned samples, which governed the specimen dimensions. Despite the absorption of up to 0.85 wt % [*I<sub>x</sub>-2<sub>y</sub>*], 1.11 wt % [*I<sub>x</sub>-3<sub>y</sub>*], and 1.46 wt % [*3<sub>x</sub>-2<sub>y</sub>*] following exposure to 75.3 % RH (> 4000 h), the samples showed no visual changes. There is a clear trend evident, with the ultimate moisture uptake rising with the quantity of **3** present in the blends; this phenomenon is observed in both the elevated humidity and direct immersion studies reported later.

Spectral analysis (FT-IR spectroscopy) was performed periodically on cured samples of [*I<sub>x</sub>-2<sub>y</sub>*] during the conditioning period to examine the nature of the moisture uptake (Figure 3).

Figure 2 Plots of mass increase (%) *versus* time for a) [*I<sub>x</sub>-2<sub>y</sub>*], b) [*3<sub>x</sub>-1<sub>y</sub>*], c) [*3<sub>x</sub>-2<sub>y</sub>*] at 75 % RH.

Figure 3 Plots of FT-IR spectra of a) cured blends of  $I_x-2_y$ , b) cured blends of  $3_x-I_y$ , c)  $I_x-2_y$  analysed periodically during 1680 hours exposure to 75 % RH.

The characteristic increase in the O-H stretching band at  $3400-3500\text{ cm}^{-1}$  represents the ‘polymeric’ water due to hydration (*i.e.* representing a hydration shell), rather than further reaction with any unreacted monomeric species. Within the series of  $[I_x-2_y]$  copolymers the spectral data support the following trend (where  $>$  indicates ‘absorbs more moisture than’). Spectral data for the cured samples of  $[3_x-I_y]$  and  $[3_x-2_y]$  are deposited as Supplementary data (Figs S5, S6).

$$[I_{60}-2_{40}] \gg [I_{50}-2_{50}] \approx [I_{90}-2_{10}] > [I_{80}-2_{20}] \approx [I_{70}-2_{30}]$$

This suggests that the reduction in moisture is not simply a function of the concentration of a more hydrophobic monomer in the blend, but perhaps by the formation of more complex molecular architectures formed in the polymerisation of CEs. It has been found by experimentation that blends containing the oligomeric phenolic CEs display much higher cross link densities than their bisphenyl type counterparts [10]. The increased numbers of cross links, calculated from DMTA data, prevent the egress of absorbed moisture through acting both as a physical barrier and also increasing the tortuosity of routes for egress of water out of the material, essentially trapping it within the voids of the cured network. Conversely, the more open structures formed through polymerization of bisphenyl based CEs enable facile ingress and egress of moisture resulting in lower net values of moisture absorption. Guenther *et al.* [13] prepared a series of CE co- and terpolymers comprising di- and tri-functional monomers (two of the monomers studied here, **1** and **2**) to study the effects of molecular architecture, catalysis and particularly free volume, on moisture uptake following a 96-hour exposure to boiling water. The methodology was very carefully designed to facilitate the careful determination of the  $T_g$  using TMA, allowing for thermal lag and drying of the ‘wet’ sample during the analysis. Guenther *et al.* found that the incorporation of even modest amounts of catalyst (*e.g.* 160 ppm Cu(II) as  $\text{Cu}(\text{acac})_2$  with nonylphenol, 1.9 phr) caused a significant reduction in the  $T_g$  (51 K) of the cured sample of **2**, following exposure to boiling water (96 hours). By way of comparison, in the present work 200 ppm Cu(II) was used as  $\text{Cu}(\text{acac})_2$  with dodecylphenol, 1 wt%.

**Determination of Water Absorption following immersion.** The full series of similar cured CE copolymers were dried to a constant weight *in vacuo* at  $60\text{ }^\circ\text{C}$  before being immersed in distilled water ( $100\text{ cm}^3$ ) for over 14000 hours at  $20\text{ }^\circ\text{C}$  with periodic removal for weighing and spectroscopic analysis. The data for each series of copolymers following immersion are shown in

Figure 4 (a)-(c); in each case the full data set is presented with the data for the initial period (Figs **S7-S9**) along with the tabulated changes in sample masses (Table **S2**) supplied as Supplementary information. Once again, none of the samples reach full equilibrium, but the absorption ranges up to 1.89 wt % [**I<sub>x-2y</sub>**], 3.03 wt % [**3<sub>x-1y</sub>**], and 3.07 wt % [**3<sub>x-2y</sub>**].

Figure 4 Mass increase (%) *versus* time for direct immersion, a) [**I<sub>x-2y</sub>**], b) [**3<sub>x-1y</sub>**], c) [**3<sub>x-2y</sub>**]

CEs are well known for their characteristic low moisture absorption [14,15] when immersed in water or exposed to humid environments.

**Determination of thermal stability following moisture conditioning.** From the data obtained from thermogravimetric analysis (TGA), there appears to be little difference in the onset of the thermal degradation (Table 2), although the influence on the thermo-mechanical properties (the ‘hot/wet’ characteristics) is more profound.

Table 2 Onset of thermal degradation for cured binary cyanate ester blends as determined by TGA before and after conditioning (nitrogen, 10 K/minute)

The full set of thermal data acquired for the neat homo- and copolymers (prior to conditioning) are included in the Supplementary information (Table **S3**). This is shown graphically for a selected blend, [**3<sub>50-150</sub>**] before and after exposure to 75 % RH (Figure 5). Analysis of the conditioned samples using DMTA shows that both the magnitude of the modulus and the position of the glass transition are reduced (Fig. **S11**), with the immersion conditions causing the greatest reductions in both parameters. This is shown clearly in Table 3, which details the effects of the moisture conditioning on the full set of blend samples.

Figure 5 Comparison of TGA data for unexposed (red) and exposed (black) for the blend [**3<sub>50-150</sub>**]

Table 3 Thermomechanical data for cured binary cyanate ester blends following exposure to different conditioning regimes

The DMTA data (Fig. **S12**) yield interesting information about the crosslinked structure. The breadth of the  $\tan \delta$  peaks show differences in the damping behaviour of the CEs and the peak widths represent the temperature ranges over which the glass transition temperatures occur. Thus, the  $\tan \delta$  peak recorded for **I<sub>70-230</sub>** becomes significantly more bimodal following exposure to 75 %

RH for 4000 hours to form [I<sub>70</sub>-2<sub>30</sub>]. This can be attributed to more heterogeneous networks containing both highly- and less densely crosslinked regions [16] consistent with hydrolysis of covalent bonds. This, in turn, results in a broad distribution of molecular mobilities or relaxation times. The cross link density ( $\nu$ ) for each CE copolymer was calculated from the DMTA data using equation (1) [17]. This equation is technically most appropriate for lightly cross-linked materials so it should only be used as a comparison between similar materials.

$$\nu = G_e / \phi RT_e \quad (\text{eqn 1})$$

Where  $\phi$  is taken as unity,  $G_e$  is the storage modulus strictly from a sample at equilibrium, but is taken at  $T_e$ , where  $T_e = (T_g + 50 \text{ K})$ .

The crosslink density values are shown for the CE copolymers as initially polymerized (denoted ‘virgin sample’) and following conditioning at 75 % RH and following direct immersion in water (Table 4). Examination of the data for the virgin CEs indicates that the copolymers based on I<sub>x</sub>-2<sub>y</sub> develop similar levels of crosslink density (4-7 molcm<sup>-3</sup>), whereas significantly higher crosslink densities are developed for copolymers comprising either 3<sub>x</sub>-I<sub>y</sub> (41-95 molcm<sup>-3</sup>), or for 3<sub>x</sub>-2<sub>y</sub> (53-86 molcm<sup>-3</sup>). The moisture conditioning experiments appear to have different effects on the network structures. Thus, for copolymers of I<sub>x</sub>-2<sub>y</sub> the result serves to increase the crosslink density markedly (2-6 fold); for copolymers of 3<sub>x</sub>-I<sub>y</sub> more modest increases (of up to 2-fold) are observed; for copolymers of 3<sub>x</sub>-2<sub>y</sub> the crosslink density increases slightly, or decreases slightly. With the more forcing immersion conditions, the crosslink density generally increases in the case of the copolymers based on difunctional monomers, but falls significantly in the copolymers of 3<sub>x</sub>-2<sub>y</sub>, which contain oligomers of higher functionality.

Table 4 Crosslink density data for cured CE copolymers as determined by DMTA following exposure to different moisture conditioning regimes

Although the situation is clearly both complex and dynamic with numerous possibilities, the initial depth of moisture ingress into the polymer and its resultant effect on the polymer chain interactions appear to be a key influence on the propensity of the CE to yield carbamate *via* the accepted mechanism [18] involving slow formation of an imidocarbonate (catalyzed by residual metal ions present in the polymerization catalyst), and fast rearrangement to form a carbamate, which can undergo decarboxylation at typical cure temperatures or soldering processes (Scheme 1).



Scheme 1 Degradation of partially cured CE polymers *via* carbamate formation and decarboxylation.

The DMTA data support the hypothesis that copolymers based on [ $I_x-2_y$ ] are more lightly crosslinked when compared to those of [ $3_x-I_y$ ] and [ $3_x-2_y$ ]. We suggest that this light crosslinking facilitates the ingress of moisture further into the cured polymer where water interacts with the polymer chains (acting as a hydrogen donor), thus increasing the crosslink density following conditioning (Scheme 2), however this must remain a working hypothesis at this stage and work is now underway to examine this phenomenon with analytical techniques that are sensitive to surface features.

Scheme 2 Influence of network crosslink density on moisture ingress and egress or degradation mechanisms.

The egress of moisture is thus compromised by a path of increasing tortuosity, compounded by an increased depth in comparison with the other blends. A similar explanation may be offered in copolymers of [ $3_x-I_y$ ], in which although the initial crosslink density is a little higher it is of the same order of magnitude (restricting ingress to similar depths and resulting in increasing crosslinking on exposure). Importantly, the retention of moisture within the bulk polymer leads to slow carbamate formation and decarboxylation on heating to elevated temperatures above 200 °C (Scheme 1), causing blistering. However, a different scenario is envisaged for copolymers of [ $3_x-2_y$ ], particularly those in which component **3** predominates. The virgin copolymers of  $3_x-I_y$  display the highest crosslink densities of the samples examined here, which would limit the depth of moisture ingress (and carbamate formation). However, upon exposure the reduction in crosslink density observed could allow the egress of absorbed moisture as the temperature is increased with the regression path becoming more open. This would, in turn, facilitate the loss of moisture prior to decarboxylation. To demonstrate the results of outgassing further in the CE copolymers, high-resolution images were acquired of [ $I_{50}-2_{50}$ ] following immersion testing and DMTA measurements to show the resulting structural deformation (Fig. **S13**).

Accelerated temperature testing (immersion in boiling water for 14 days) was performed on all the homopolymers and selected copolymers and the data are also presented in Table 2. These samples were examined closely for physical changes in appearance, structural integrity, thermal stability and dynamic mechanical thermal properties. Although there is a significant reduction in  $T_g$  for all blends when subjected to accelerated ageing (by immersion at 100 °C, Table 2), the reduction in ‘outgassing’ (due to the evolution of carbon dioxide following decarboxylation of the carbamate, Scheme 1) is significantly reduced in copolymer combining **2** and **3** when compared with the homopolymers or the

other copolymers (Fig. S14). The thermal behaviour of the copolymer comprises elements of both networks of the neat polymers: displaying a flatter response at lower temperatures (where the behaviour of **2** predominates), but appears more similar to **1** at higher temperatures, suggesting that this component exerts a greater influence over the degradation as it possesses the weaker linkages.

**Examination of the effects of long term immersion in highly acidic and basic media.** The cured samples were also immersed in acidic and basic media (for a total of 3000 hours). Somewhat surprisingly, the mass changes in the immersed samples were practically identical (+1.01-1.02 %) over the timescale (Table S4), although the initially colourless basic solution became progressively more straw coloured with the presence of small fragments of solid suspended within it (Fig. S15, top), shown for [3<sub>80</sub>-2<sub>10</sub>]. This corresponded to marked etching apparent on the surface of the sample (also [3<sub>80</sub>-2<sub>20</sub>]) (Fig. S15, bottom).

The results of the analysis of the blend [I<sub>50</sub>-2<sub>50</sub>] using DMTA following exposure either to water, sulphuric acid, or sodium hydroxide is shown in Fig. 9 and Table 5. These data show clearly that the different media have subtly different effects. For example, the magnitude of the modulus is most clearly affected most by the introduction of water (lubrication) or sodium hydroxide, whereas acid has much less effect in this regard. However, the situation is reversed when examining the position of the glass transition (related to free volume or crosslink density) with immersion in the acid causing the greatest reduction in this parameter (albeit a relatively small reduction).

Table 5 Thermomechanical data for cured CE copolymers following exposure to different conditioning regimes

Figure 6 DMTA comparison of [I<sub>50</sub>-2<sub>50</sub>] immersed in water (black), H<sub>2</sub>SO<sub>4</sub> (red) and NaOH (blue).

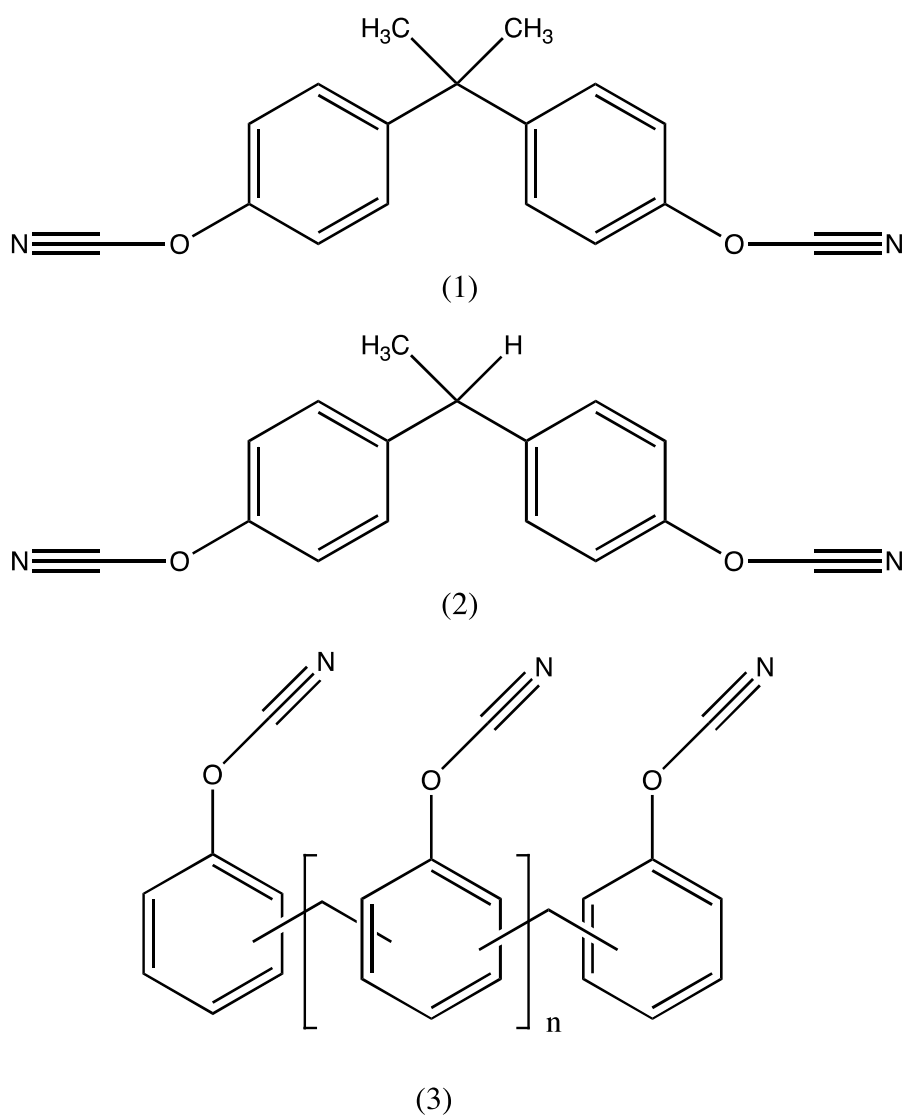
## CONCLUSIONS

The combination of polycyanurates to form co-polymeric networks appears to have been examined only sparingly in the research literature, despite the comparative simplicity and versatility of the approach. The results of the present study have demonstrated the beneficial thermal and mechanical properties that can be achieved through reactive blending of this kind to yield novel materials. From a processing perspective the combination of even comparatively small quantities of the liquid monomer **2** serve to improve the flow of both monomer **1** and the oligomer **3**. In the case of the more highly aromatic **3**, this yields a copolymer with significantly improved thermal properties (*i.e.* greatly increased  $T_g$  over **1**) with greatly improved processing characteristics. The significant reduction in outgassing observed in blends containing **3** and **2**, particularly **3**<sub>90</sub>-**2**<sub>10</sub>, offers a marked improvement in comparison with the homopolymers and other cyanate ester copolymers.

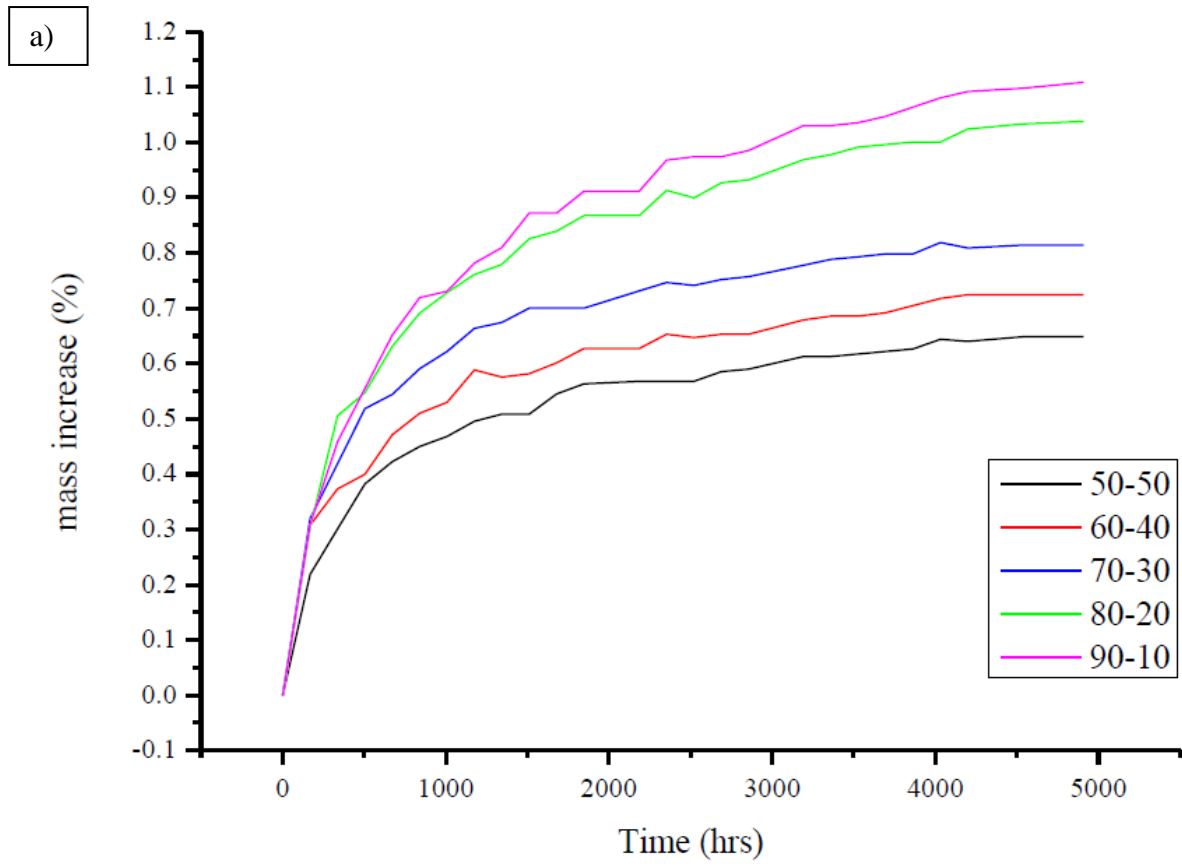
## REFERENCES

- (1) Hamerton, I.; Mooring, L. The use of thermosets in aerospace applications, Chapter 7 in *Thermosets Structure, Properties and Applications*, Qipeng Guo (Ed.) Woodhead Publishing: Cambridge, **2012**, pp. 189-227.
- (2) *Chemistry and Technology of Cyanate Ester Resins*, I Hamerton (Ed.), Blackie A&P; Glasgow, **1994**.
- (3) Tao, Q.S.; Gan, W.J.; Yue, Y.F.; Wang, M.H.; Tang, X.L.; Li, S.J. *Polymer*, **2004**, *45*, 3505-3510.
- (4) Suman, J.; Kathi, J.; Tammishetti, S. *Euro. Polym. J.*, **2005**, *41*, 2963-2972.
- (5) Nair, C.P.R.; Mathew, D.; Ninan, K. *Cyanate Ester Resins, Recent Developments, New Polymerization Techniques and Synthetic Methodologies*, **2001**, Springer: Berlin, pp. 1-99.
- (6) Karad, S.K.; Attwood, D.; Jones, F.R. *Composites Part A*, **2002**, *33*, 1665-1675.
- (7) Leach, D.; Boyd, J. *Proc. 46<sup>th</sup> Int. SAMPE Symp. Exhib.*, **2001**, SAMPE, Long Beach, 1506-1514.
- (8) Nair, C.P.R.; Vijayan, F.T.; Krishnan, K. *J. Appl. Polym. Sci.*, **1999**, *74*, 2737-2746.
- (9) McConnell, V.P., *Advanced Composites*, **1992** (May/June) p. 28.

- (10) Bishop, J. *Handbook of Adhesives and Sealants*, P. Cognard (Ed.) **2005**, Elsevier, p. 319.
- (11) Crawford, A.O.; Howlin, B.J.; Cavalli, G.; Hamerton, I. *React. Func. Polym.*, **2012**, *72*, 595-605.
- (12) Greenspan L. Humidity fixed points of binary saturated aqueous solutions, *National Bureau of Standards A*, **1977**, *81*, A(1).
- (13) Guenther, A.; Yandek, G.; Mabry, J.; Lamison, K.; Vij, V.; Davis, M.; Cambrea, L. Insights into moisture uptake and processability from new cyanate ester monomer and blend studies, *SAMPE Fall Tech. Conf.* 2010, Salt Lake City, UT, 11-14 October 2010.
- (14) Shimp, D.A.; Christenson, J.R.; Ising, S.J. *34th Int. SAMPE Symp. Exhib.*, **1989**, 222.
- (15) Bogan, G.W. *SAMPE J.*, 1988, *24*, 19.
- (16) Kannurpatti, A.R.; Anseth, J.W.; Bowman, C.N. *Polymer*, **1998**, *39*, 2507-2513.
- (17) Allen, D.J.; Ishida, H. *J. Appl. Polym. Sci.*, **2006**, *101*, 2798–2809.
- (18) *Chemistry and Technology of Cyanate Ester Resins*, I Hamerton (Ed.), Blackie A&P; Glasgow, **1994**, pp. 116-118.



**Figure 1** Cyanate ester structures studied in this work (*N.B.*, in this instance  $n = 1$  in structure 3)



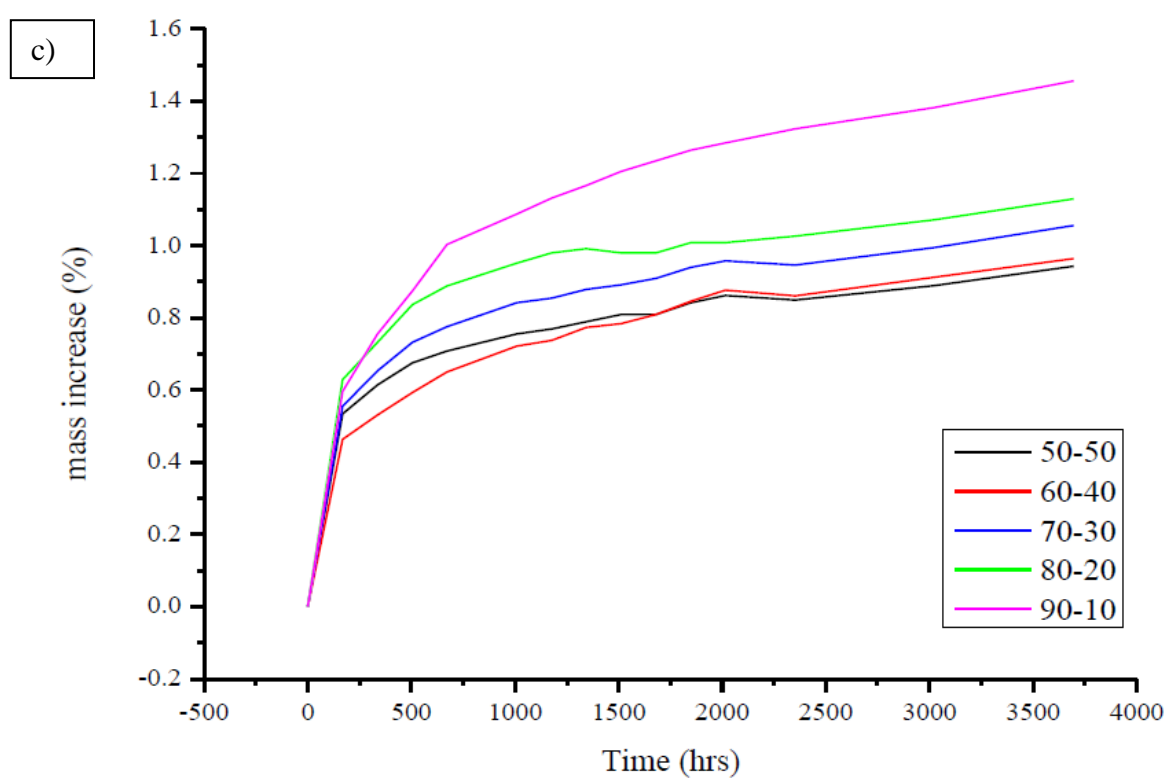
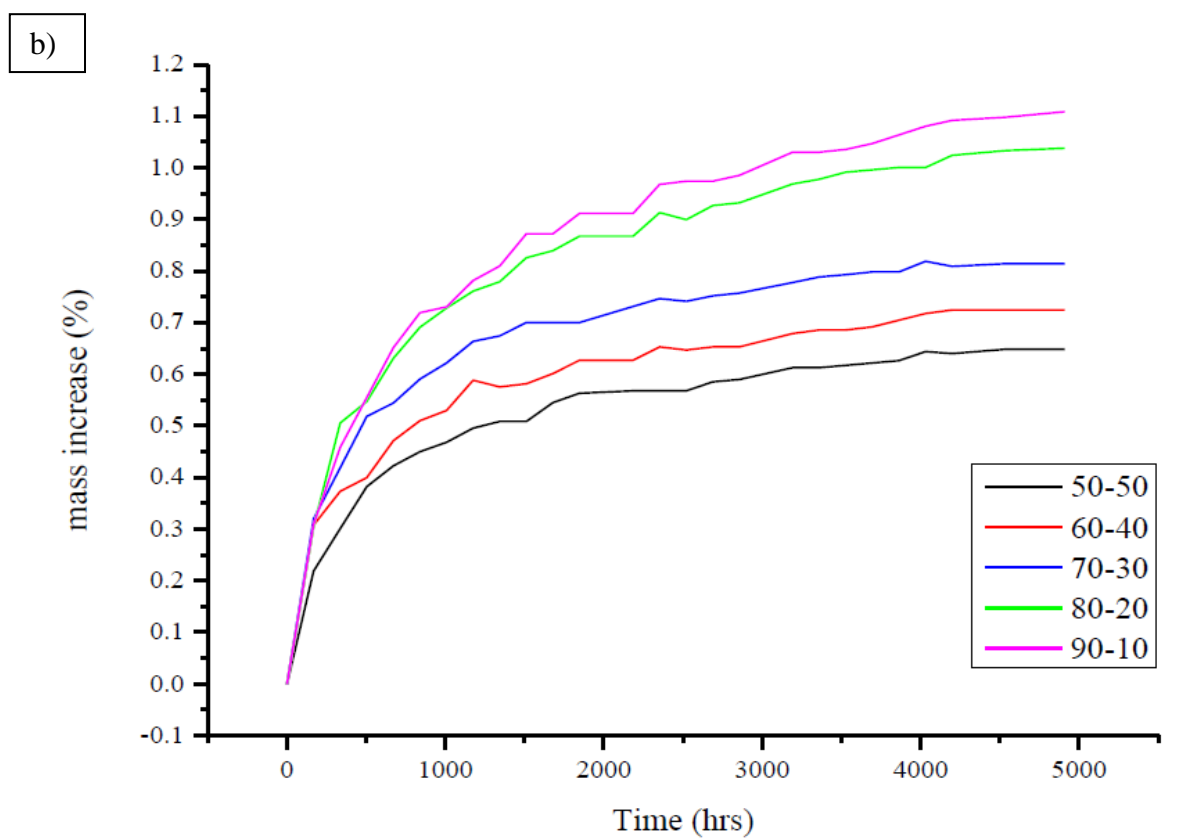
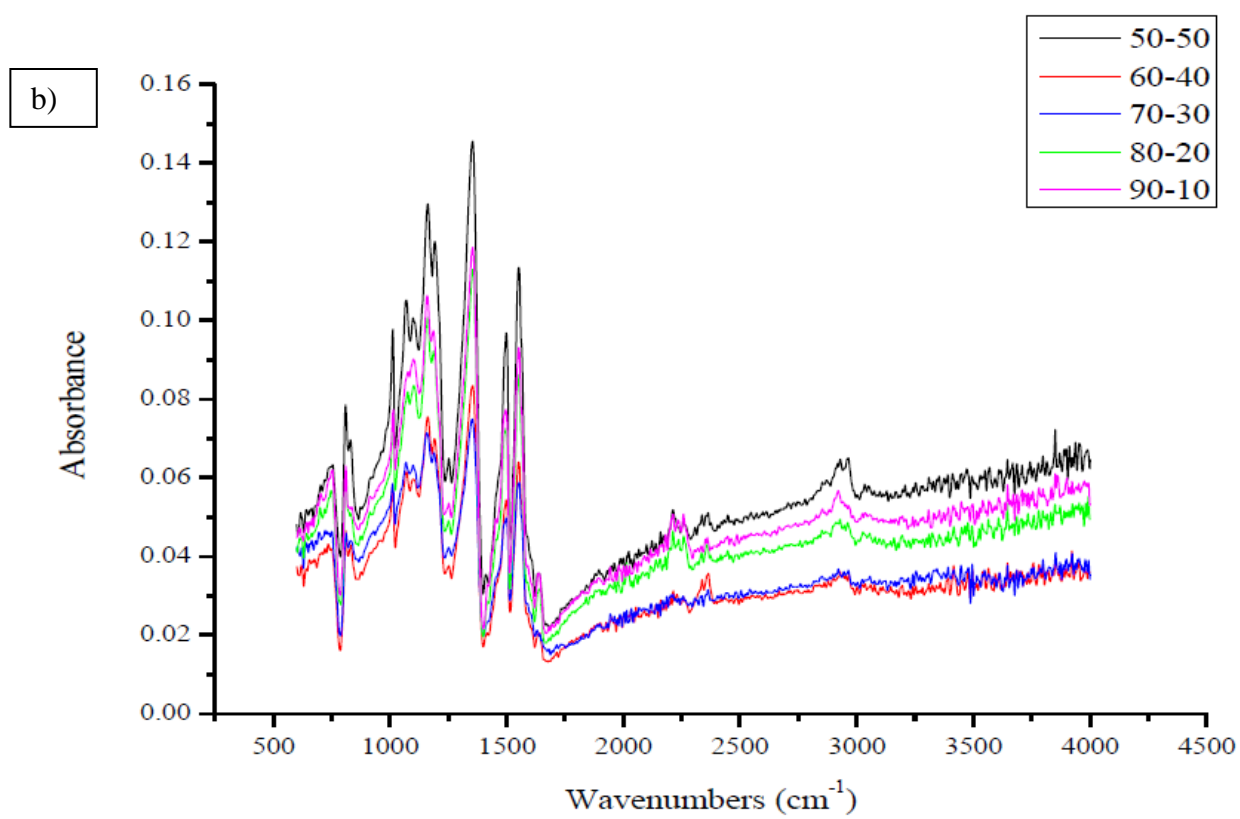
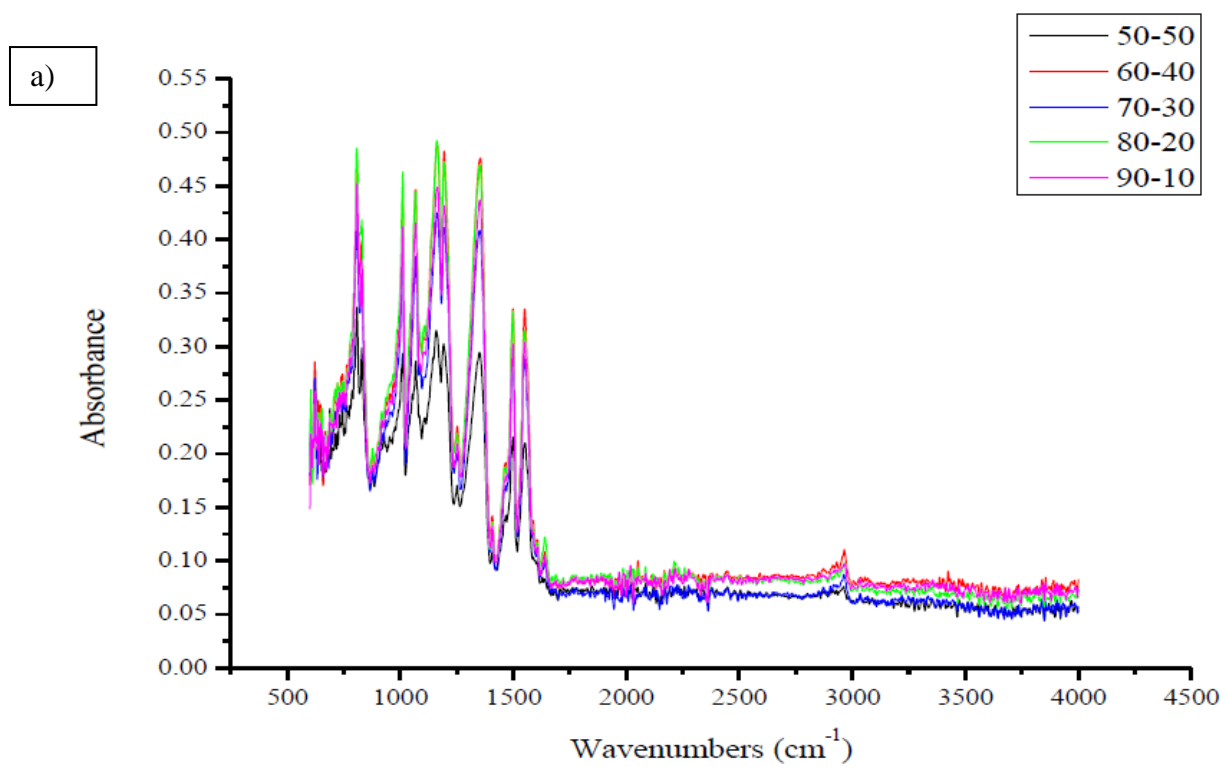
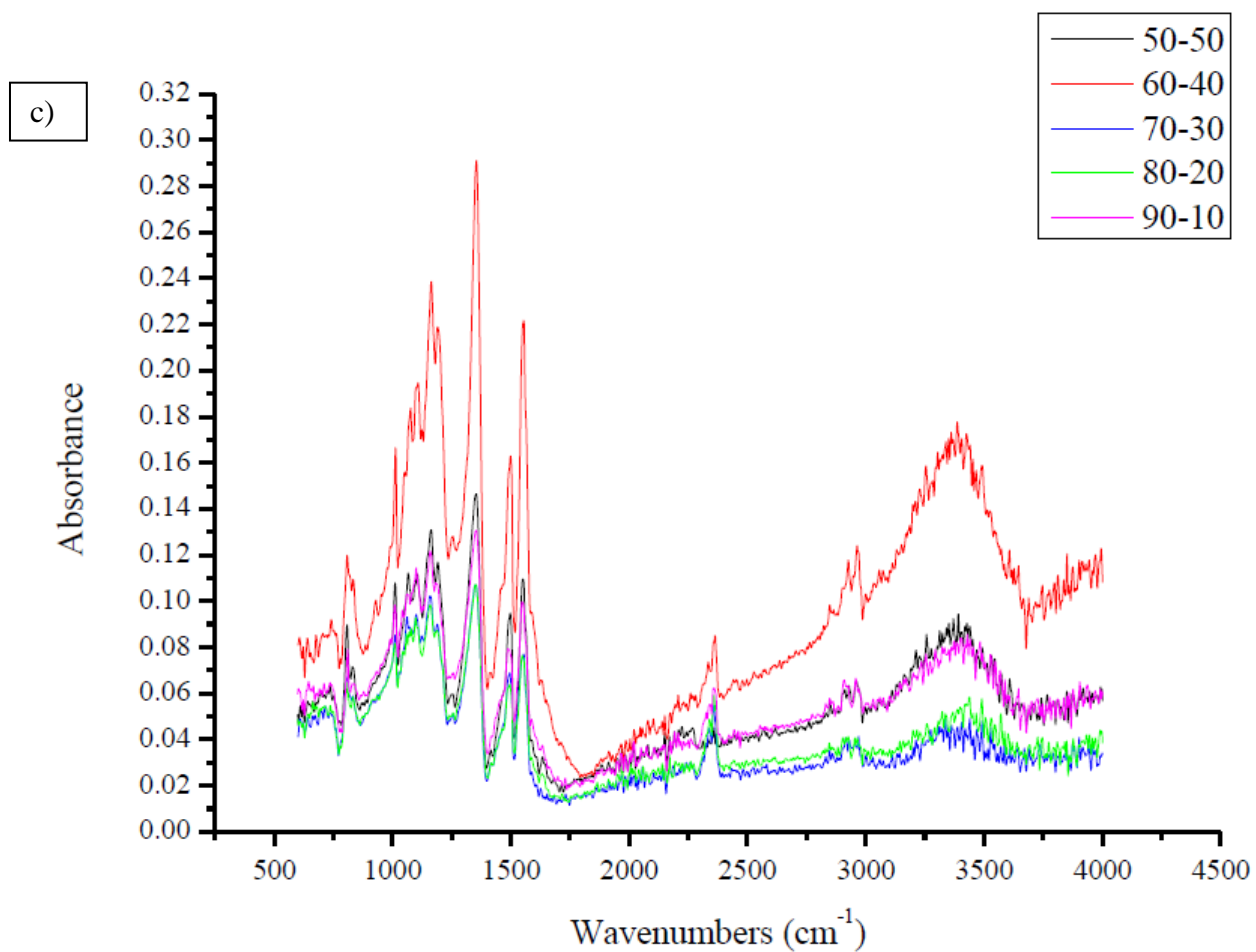


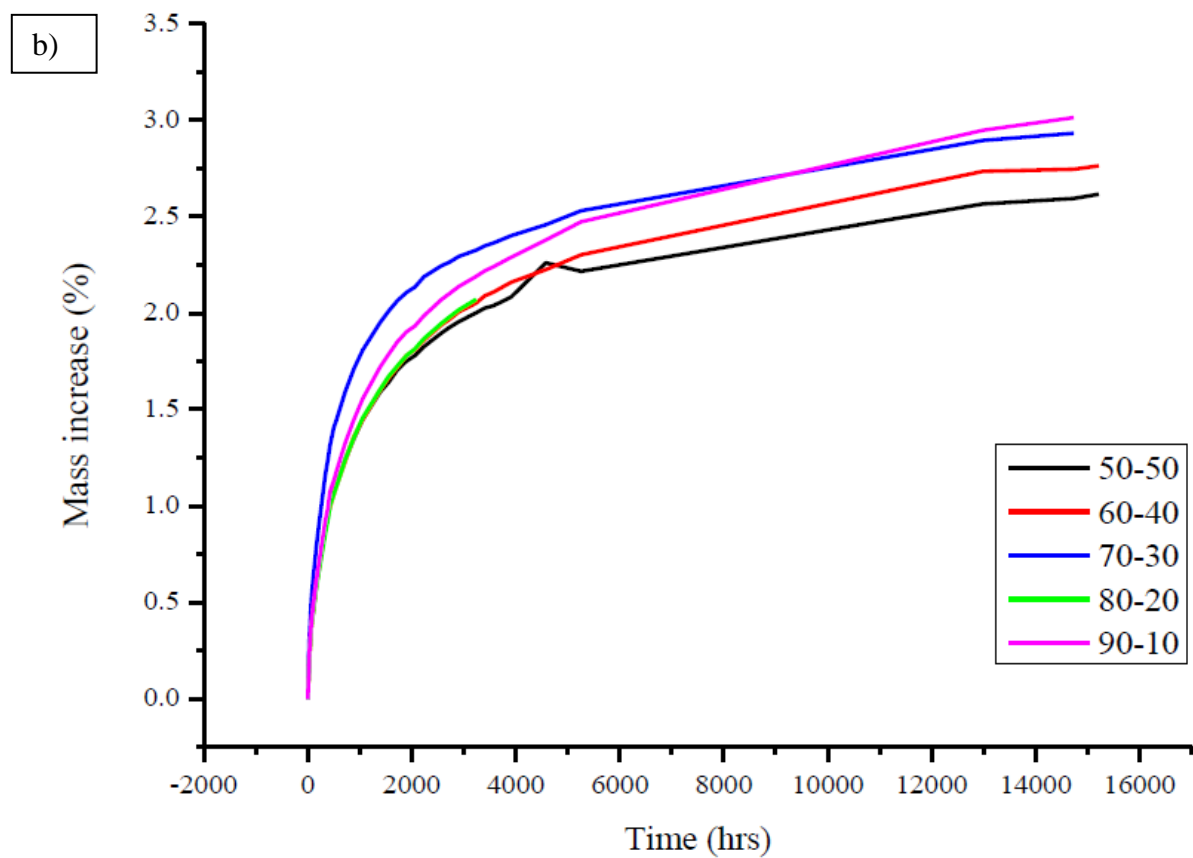
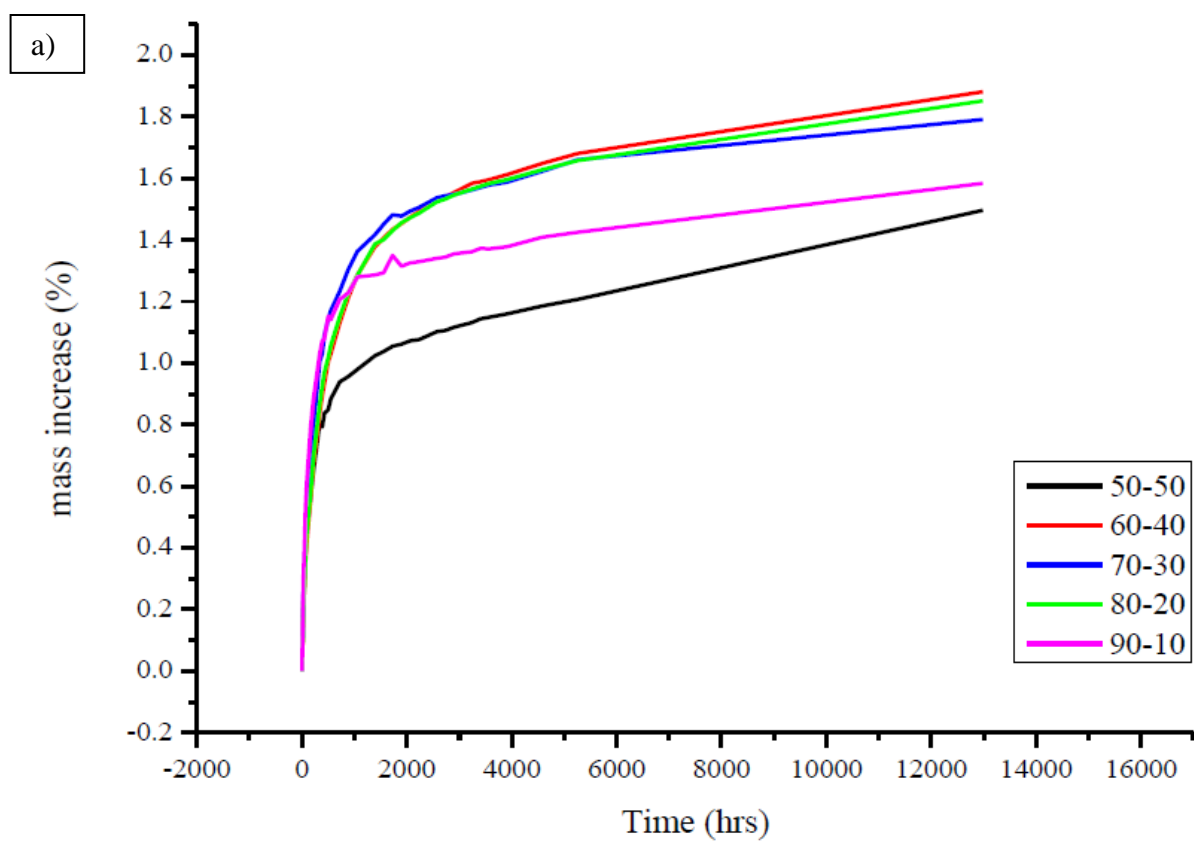
Figure 2 Plots of mass increase (%) versus time for a)  $[1_x-2_y]$ , b)  $[3_x-1_y]$ , c)  $[3_x-2_y]$  at 75 % RH.







**Figure 3** Plots of FT-IR spectra of a) cured blends of  $I_x-2y$ , b) cured blends of  $3x-I_y$ , c)  $I_x-2y$  analysed periodically during 1680 hours exposure to 75 % RH.



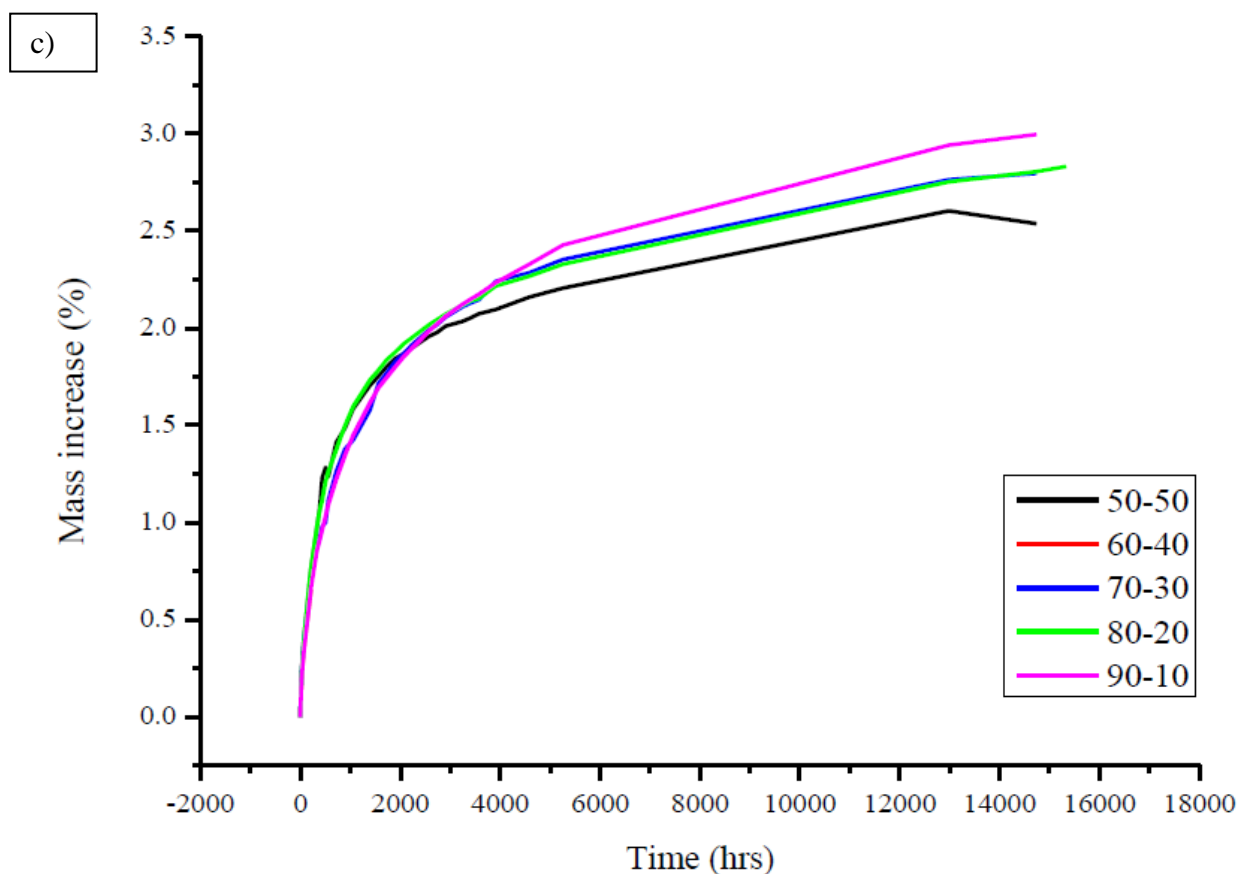


Figure 4 Mass increase (%) versus time for direct immersion, a)  $[1_x-2_y]$ , b)  $[3_x-1_y]$ , c)  $[3_x-2_y]$

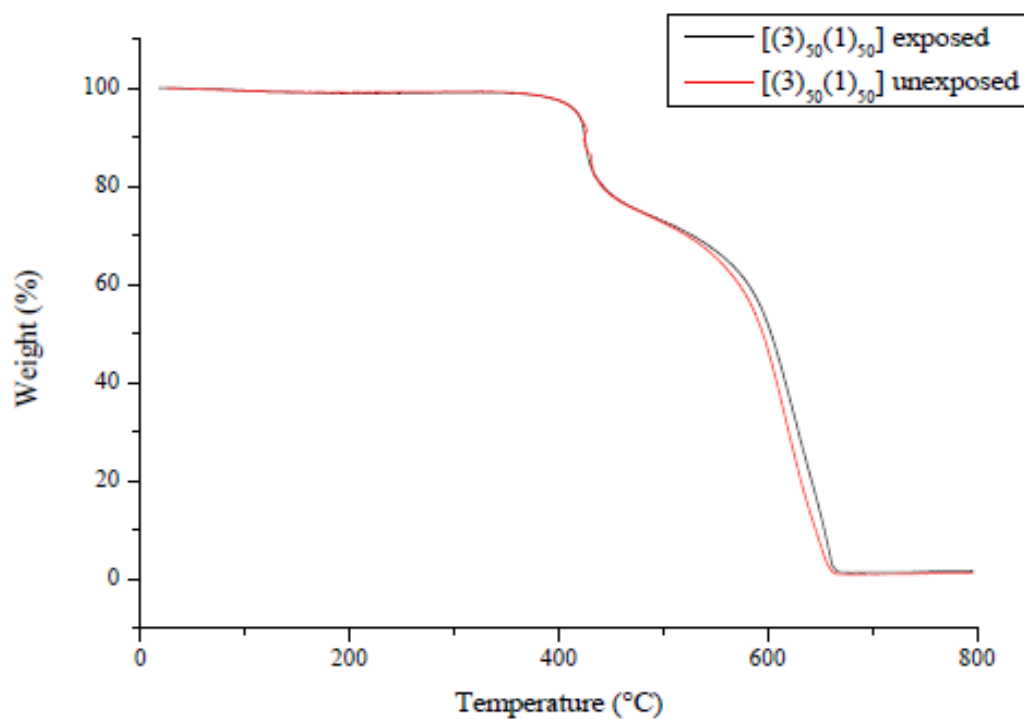
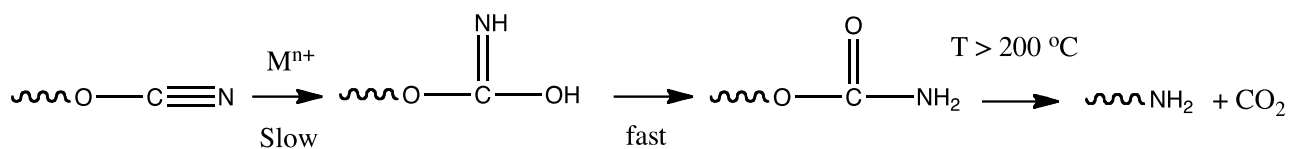
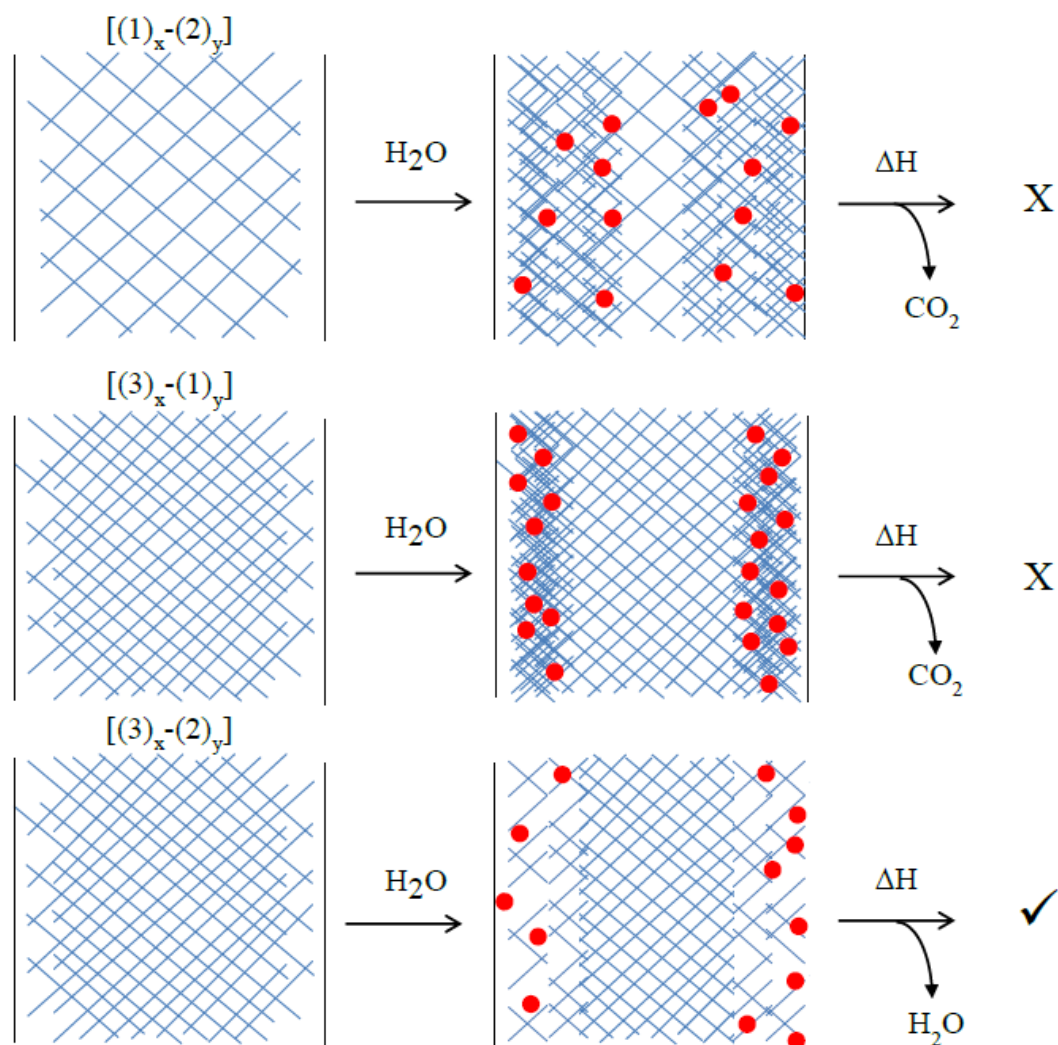


Figure 5 Comparison of TGA data for unexposed (red) and exposed (black) for the blend  $[3_{50}-1_{50}]$



**Scheme 1** Degradation of partially cured CE polymers *via* carbamate formation and decarboxylation.



**Scheme 2** Influence of network crosslink density on moisture ingress and egress or degradation mechanisms.

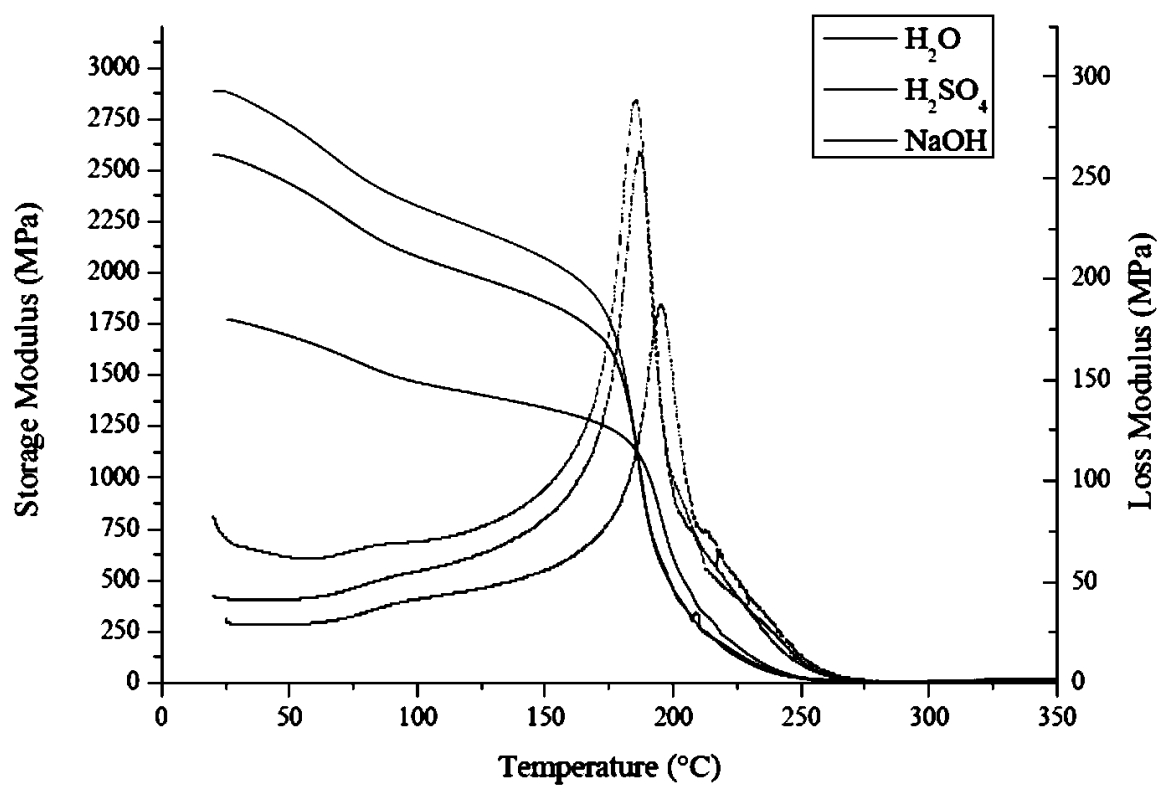


**Figure 6** DMTA comparison of  $[I_{50-250}]$  immersed in water (black), H<sub>2</sub>SO<sub>4</sub> (red) and NaOH (blue).

Table 1 Designation of monomers and blends examined in this work

Sample Designation	Cyanate Ester		
	1	2	3
<b>1</b>	100	0	0
<b>2</b>	0	100	0
<b>3</b>	0	0	100
<b>1<sub>50</sub>-2<sub>50</sub></b>	50	50	0
<b>1<sub>60</sub>-2<sub>40</sub></b>	60	40	0
<b>1<sub>70</sub>-2<sub>30</sub></b>	70	30	0
<b>1<sub>80</sub>-2<sub>20</sub></b>	80	20	0
<b>1<sub>90</sub>-2<sub>10</sub></b>	90	10	0
<b>3<sub>50</sub>-1<sub>50</sub></b>	50	0	50
<b>3<sub>60</sub>-1<sub>40</sub></b>	40	0	60
<b>3<sub>70</sub>-1<sub>30</sub></b>	30	0	70
<b>3<sub>80</sub>-1<sub>20</sub></b>	20	0	80
<b>3<sub>90</sub>-1<sub>10</sub></b>	10	0	90
<b>3<sub>50</sub>-2<sub>50</sub></b>	0	50	50
<b>3<sub>60</sub>-2<sub>40</sub></b>	0	40	60
<b>3<sub>70</sub>-2<sub>30</sub></b>	0	30	70
<b>3<sub>80</sub>-2<sub>20</sub></b>	0	20	80
<b>3<sub>90</sub>-2<sub>10</sub></b>	0	10	90

**Key** the composition of the blend is indicated by the subscript. Thus, a blend comprising 90 % of monomer 1 and 10% of monomer 2 is denoted **1<sub>90</sub>-2<sub>10</sub>**. Cured blends are denoted by the use of italics to differentiate them from the corresponding monomer blend *i.e.* monomer blend **1<sub>90</sub>-2<sub>10</sub>** becomes polycyanurate *I*<sub>90-210</sub> following cure. Following conditioning, parentheses are added: [*I*<sub>90-210</sub>]

Table 2 Onset of thermal degradation for cured binary cyanate ester blends as determined by TGA before and after conditioning (nitrogen, 10 K/minute)

Copolymer	Virgin Sample	75 % RH	Direct Immersion
[I <sub>50</sub> -2 <sub>50</sub> ]	414	414	414
[I <sub>60</sub> -2 <sub>40</sub> ]	411	410	409
[I <sub>70</sub> -2 <sub>30</sub> ]	416	414	415
[I <sub>80</sub> -2 <sub>20</sub> ]	413	412	413
[I <sub>90</sub> -2 <sub>10</sub> ]	410	409	409
[3 <sub>50</sub> -I <sub>50</sub> ]	416	415	413
[3 <sub>60</sub> -I <sub>40</sub> ]	419	417	418
[3 <sub>70</sub> -I <sub>30</sub> ]	420	419	418
[3 <sub>80</sub> -I <sub>20</sub> ]	420	416	415
[3 <sub>90</sub> -I <sub>10</sub> ]	419	415	412
[3 <sub>50</sub> -2 <sub>50</sub> ]	420	419	418
[3 <sub>60</sub> -2 <sub>40</sub> ]	420	418	420
[3 <sub>70</sub> -2 <sub>30</sub> ]	408	408	410
[3 <sub>80</sub> -2 <sub>20</sub> ]	420	418	419
[3 <sub>90</sub> -2 <sub>10</sub> ]	418	417	418

*N.B.*, the onset of degradation was determined by the temperature at which a mass loss of 5% was recorded.

Table 3 Thermomechanical data for cured binary cyanate ester blends following exposure to different conditioning regimes

Sample	Virgin sample			75 % RH			Direct immersion H <sub>2</sub> O (25 °C)			Direct immersion H <sub>2</sub> O (100 °C)		
	$E'_{25^{\circ}\text{C}}$ (MPa)	$E''_{\text{max}}$ (°C)	$\text{Tan}\delta_{\text{max}}$ (°C)	$E'_{25^{\circ}\text{C}}$ (MPa)	$E''_{\text{max}}$ (°C)	$\text{Tan}\delta_{\text{max}}$ (°C)	$E'_{25^{\circ}\text{C}}$ (MPa)	$E''_{\text{max}}$ (°C)	$\text{Tan}\delta_{\text{max}}$ (°C)	$E'_{25^{\circ}\text{C}}$ (MPa)	$E''_{\text{max}}$ (°C)	$\text{Tan}\delta_{\text{max}}$ (°C)
<b>1</b>	2782	301	315	-	-	-	-	-	-	2221	150	187
<b>2</b>	-	-	-	-	-	-	-	-	-	2292	159	180
<b>3</b>	3294	-	-	-	-	-	-	-	-	2891	178	220
<b>I<sub>50</sub>-2<sub>50</sub></b>	2087	241	288	2012	209	267	1772	195	252	-	-	-
<b>I<sub>60</sub>-2<sub>40</sub></b>	2207	254	296	1940	220	278	2343	188	248	-	-	-
<b>I<sub>70</sub>-2<sub>30</sub></b>	2603	255	293	2238	219	277	2090	190	252	-	-	-
<b>I<sub>80</sub>-2<sub>20</sub></b>	2498	250	291	2396	222	277	2075	190	252	-	-	-
<b>I<sub>90</sub>-2<sub>10</sub></b>	1917	258	287	1739	227	278	2464	196	253	-	-	-
<b>3<sub>50</sub>-I<sub>50</sub></b>	2719	318	347	2283	269	294	2912	210	-	-	-	-
<b>3<sub>60</sub>-I<sub>40</sub></b>	2757	317	342	2481	247	286	2544	211	-	-	-	-
<b>3<sub>70</sub>-I<sub>30</sub></b>	2382	-	-	2851	251	288	3260	213	246	2361	151	184
<b>3<sub>80</sub>-I<sub>20</sub></b>	2792	325	-	2492	296	320	2609	207	241	-	-	-
<b>3<sub>90</sub>-I<sub>10</sub></b>	3004	-	-	2481	270	292	2923	208	245	2841	134	157
<b>3<sub>50</sub>-2<sub>50</sub></b>	2543	306	337	2681	251	316	2009	209	243	2617	144	170
<b>3<sub>60</sub>-2<sub>40</sub></b>	2554	306	330	2742	246	297	2641	206	241	-	-	-
<b>3<sub>70</sub>-2<sub>30</sub></b>	2589	309	332	2058	249	275	2488	209	244	-	-	-
<b>3<sub>80</sub>-2<sub>20</sub></b>	2420	303	331	3004	247	294	2581	209	247	3073	133	157
<b>3<sub>90</sub>-2<sub>10</sub></b>	2523	-	-	2596	252	291	2694	211	256	-	-	-

$E'_{25^{\circ}\text{C}}$  = storage modulus recorded at 25 °C,  $E''_{\text{Max}}$  = Temperature of peak maximum in loss modulus data,  $\text{Tan}\delta_{\text{max}}$  = Temperature of peak maximum in Tangent  $\delta$  data, - no data available



Table 4 Crosslink density data for cured CE copolymers as determined by DMTA following exposure to different moisture conditioning regimes

Copolymer	Virgin sample			75 % RH			Direct immersion (25 °C)		
	$T_e$ (°C)	$G_e$ (MPa)	$\nu$ (molcm <sup>-3</sup> )	$T_e$ (°C)	$G_e$ (MPa)	$\nu$ (molcm <sup>-3</sup> )	$T_e$ (°C)	$G_e$ (MPa)	$\nu$ (molcm <sup>-3</sup> )
<b><i>1</i><sub>50-2</sub><i>50</i></b>	290.3	34.3	7.3	258.3	70.6	15.9	245.3	40.4	9.4
<b><i>1</i><sub>60-2</sub><i>40</i></b>	303.8	25.2	5.3	259.3	146.1	33.0	237.8	58.0	13.7
<b><i>1</i><sub>70-2</sub><i>30</i></b>	303.8	29.1	6.1	268.9	98.6	21.9	239.8	68.4	16.0
<b><i>1</i><sub>80-2</sub><i>20</i></b>	300.1	29.8	6.3	272.0	77.2	17.0	240.2	60.6	14.2
<b><i>1</i><sub>90-2</sub><i>10</i></b>	307.6	18.5	3.8	276.4	35.8	7.8	245.5	66.9	15.5
<b><i>3</i><sub>50-1</sub><i>50</i></b>	367.7	215.0	40.7	319.2	286.1	58.1	259.8	215.7	48.7
<b><i>3</i><sub>60-1</sub><i>40</i></b>	366.7	301.7	56.7	298.5	645.1	135.7	261.0	227.4	51.2
<b><i>3</i><sub>70-1</sub><i>30</i></b>	-	-	-	301.2	521.6	109.2	263.6	316.4	70.9
<b><i>3</i><sub>80-1</sub><i>20</i></b>	375.1	510.6	94.8	345.7	683.0	132.7	257.0	248.9	56.5
<b><i>3</i><sub>90-1</sub><i>10</i></b>	-	-	-	319.3	442.4	89.8	-	-	-
<b><i>3</i><sub>50-2</sub><i>50</i></b>	356.8	248.2	54.3	301.2	386.7	80.9	259.2	132.6	29.9
<b><i>3</i><sub>60-2</sub><i>40</i></b>	356.8	402.9	76.9	296.3	343.0	72.4	255.7	222.2	50.5
<b><i>3</i><sub>70-2</sub><i>30</i></b>	358.3	280.0	53.3	299.3	206.9	43.4	259.7	192.6	43.5
<b><i>3</i><sub>80-2</sub><i>20</i></b>	353.5	449.9	86.4	-	-	-	259.7	248.1	56.0
<b><i>3</i><sub>90-2</sub><i>10</i></b>	-	-	-	-	-	-	261.4	221.8	49.9

Key:  $T_e = (T_g + 50 \text{ K})$ ,  $G_e$  = storage modulus strictly from a sample at equilibrium,  $\nu$  = crosslink density, - no data available

Table 5 Thermomechanical data for cured CE copolymers following exposure to different conditioning regimes

Sample	Direct immersion H <sub>2</sub> SO <sub>4</sub>			Direct immersion NaOH		
	$E'_{25^{\circ}\text{C}}$ (MPa)	$E''_{\text{max}}$ (°C)	$\text{Tan } \delta_{\text{max}}$ (°C)	$E'_{25^{\circ}\text{C}}$ (MPa)	$E''_{\text{max}}$ (°C)	$\text{Tan } \delta_{\text{max}}$ (°C)
<b><i>I</i><sub>50-250</sub></b>	2888	186	243	2575	188	246
<b><i>I</i><sub>60-240</sub></b>	2615	196	252	-	-	-
<b><i>I</i><sub>80-220</sub></b>	2946	189	254	2399	192	261
<b><i>I</i><sub>90-210</sub></b>	-	-	-	-	-	-
<b><i>3</i><sub>50-150</sub></b>	3150	237	-	2638	223	-
<b><i>3</i><sub>60-140</sub></b>	3066	230	-	-	-	-
<b><i>3</i><sub>70-130</sub></b>	-	-	-	3208	261	281
<b><i>3</i><sub>80-120</sub></b>	3343	227	259	-	-	-
<b><i>3</i><sub>90-110</sub></b>	3309	203	259	3339	212	-
<b><i>3</i><sub>50-250</sub></b>	3594	242	-	3260	225	-
<b><i>3</i><sub>60-240</sub></b>	3272	260	-	3781	242	-
<b><i>3</i><sub>70-230</sub></b>	2670	241	-	2476	231	270
<b><i>3</i><sub>80-220</sub></b>	2763	229	266	3325	-	-
<b><i>3</i><sub>90-210</sub></b>	3476	-	-	3169	-	-

$E'_{25^{\circ}\text{C}}$  = storage modulus recorded at 25 °C

$E''_{\text{Max}}$  = Temperature of peak maximum in loss modulus data

$\text{Tan } \delta_{\text{max}}$  = Temperature of peak maximum in Tan  $\delta$  data

- no data available